The Resistive Tubular Heater - Mathematical and Simulation Model

Mitică Iustinian Neacă

University of Craiova/Faculty of Electrical Engineering/I.E.E.A. Department
Craiova, Romania, ineaca@elth.ucv.ro

Abstract – **It is essential to achieve the mathematical model and the simulation when designing complex installations. This allows the analysis of different operating modes and the behavior of the existing system. It enables notification of possible errors and their correction, avoiding additional costs involved for achieving and testing facility in real conditions. Some operating modes could be degraded modes. This would be very difficult to replicate or would give rise to a faulty installation. In order to model and simulate a complex installation it is, however, need that the components are modeled correctly and to be interpreted correctly the interactions between them and the dependency of the parameters on the operating conditions. Because many complex systems incorporate electrical heating tube elements, this paper proposes an original mathematical model for a resistive tubular heater. Based on this model it was developed a Matlab-Simulink simulation model. The model has been designed so that it can be easily adapted to various situations, where the heating elements in tube are immersed in liquids or embedded in solid materials. The proposed model allows a fast simulation and evaluation of the function of the resistive tubular heater in transient regime or under steady state regime. One challenge was to minimize the parameters which need to be pre-calculated based on physical and constructive data, in order to enroll them in the prescription blocks of the model. The viability of the presented modeling system was verified both by comparison with a real heating element and by drawing the temperature curves. These curves highlight the fitting in the admitted temperature domain for such an element.**

Cuvinte cheie: *încălzire electrică, model matematic, model de simulare, element incalzitor rezistiv în tub.*

Keywords: *electric heating, mathematical model, simulation model, tubular resistive heater.*

I. INTRODUCTION

Many of the current equipments, whether they are for industrial or domestic use, include electric heating elements. From the various possibilities of obtaining heat by converting the electric energy, the most used in such equipments is the one based on the Joule-Lenz effect. Here, the heat is generated by passing electric current through a resistive element.

On the other hand, during operation mode, there are many devices in which the heat produced by the resistive element must be transmitted to an environment of relatively good electrical conductivity (for example: water, salt bath, etc.). In such an environment, the operation of a resistive element is not possible due to short-circuit of the conductors. In these circumstances we rely on the installa-

tion of resistive heating elements in tube. Such resistances in tube are made worldwide in a very diverse range of sizes and shapes.

In electrical heaters with visible resistances or heaters with resistors embedded in pulp ceramic insulation, the calculation of the dimensions of the heating spiral is done by specific power of the wire. Compared to these, the electric heating element in tube is dimensioned based on the specific power of the tube outer surface.

Each company producing resistive heating elements in tube has developed a computing and sizing system that takes into account the manufacturing technology, the used materials, the dimensions and forms accepted by the potential future owners. The analysis of the current offer, worldwide, shows a trend of standardization in terms of electric power turned into heat by a heating element and the physical form of the element ([1]-[7]). Regarding this last point, should be noted that there are situations in which the user acquires the linear tube and bends it according to his needs, respecting the manufacturer specifications [3].

On the other hand, in the current period, it has become inconceivable to ensure the technical progress in the absence of some viable mathematical models for various installations components. The simulations of these submodels then become parts of a complex model that allows the simulation of different operating modes for the installations as a whole. Simulation processes are very useful especially when the proposed working regime can often lead to irreparable damage of the plant.

In addition to a correct modeling of the elements, it is necessary that the designer knows or understand the interdependencies that occur between various elements of the installation as a whole. Also, mathematical models and their simulations must take into account the influences that the modification of the operating regime may have on some of the defining parameters of the model.

In [8] is partially presented a mathematical model of an electric furnace with resistances, used for heat treatments. The system is quite complex (the mathematical model of the furnace comprises 67 equations), being doubled by the automation subsystem. For this type of industrial plant there were used coiled air resistances, whose mathematical model is described in [9].

In many papers, we can find some general principles and equations regarding the heat generation, transfer and modeling ([10]-[19]). Also, it can be found different mathematical models for tube heating elements through which passes fluid thermal agent ([20]-[27]). But, we could not find a modeling system for a heating resistive element in metal tube.

This paper proposes an original model for such an element. In future work, this will allow mathematically modeling and simulating a heat treatment furnace equipped with resistive tube elements.

II. TUBULAR RESISTIVE HEATER – BUILDING SYSTEM

In Figure 1 is presented a resistive heating element in tube, from the construction point of view [6]. It can be seen that besides the area that actually produce heat, there are two end zones that allow fixing and power supplying the resistance.
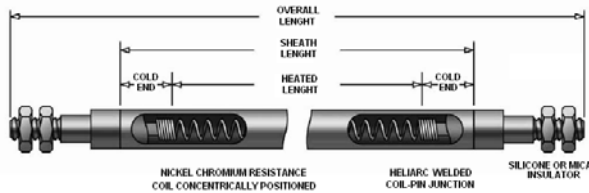

Fig. 1. Resistive element in tube [6].

Due to the big length of the core, the small diameter of the tube and the wire of which the spiral is made, it is necessary to ensure centering of the heating spiral in the metal tube. The heating spiral of the electric heater element in tube must be centered and insulated from the tube through an insulating material, in order to enable safe operation, without shock hazard to operating personnel and simultaneously to satisfy the following conditions [28]:

- to ensure the protection of the wire material against oxidant effect of air and to increase the lifetime of the heating element;
- to fix the position of the heating spiral inside the tube;
- to work at temperatures that reach 1100°C in some cases;
- to possess a thermal conductivity as high as possible in order to ensure the best possible transmission of heat from the heating coil to the environment;
- not to corrode the heating spiral or the tube material, both while working at high temperatures and at storage or stationary temperature;
- to be less hygroscopic;
- not to be injurious to workers during the manufacturing process;
- to allow the application of a productive technology in terms of guaranteed quality.

This material is introduced in granulated form during the manufacturing process. The particles and their distribution should be chosen in order to provide an uniform flow of the powder in the length of the tube and in the interior of the coil. The capacity of the insulating material and its uniformity over the whole length of the tube depends on the size and distribution of the granules, and their ability to uniformly flow while filling the tube. Figure 2 presents a detail which illustrates the components of the heating resistance [3].

Under the above aspects, the used raw materials are: oxides of magnesium, aluminum, silicon, zirconium and beryllium. The last two are less used because of their high price. Currently, magnesium oxide (magnesia) is used with priority as insulating material in the manufacture of electric heating elements in tube, due to its exceptional properties. It is a synthetic product which is characterized by a high degree of purity.
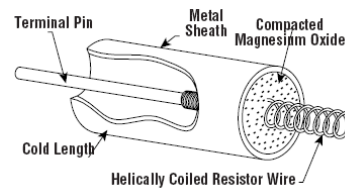

Fig. 2. Terminal detail – resistive element [3].

One clue that indicates the quality of the insulation material is the density of dust inside the tube after vibration. In the tube filled with the filling machine type Kanthal Oakley, the density of magnesium oxide of first quality is $2.40 \div 2.45$ g/cm^3. The density of the not vibrated material is $2.0 \div 2.1$ g/cm^3. Filling and closing the tube is followed by the operation of reduction of the tube section by pressing it. The mechanical strength of the tube material limits the density of the powder that can be obtained by compression. After compression, the density of the dust needs to increase up to $3.05 \div 3.15$ g/cm^3, so that the electrical tube heating elements can be used without danger in high temperature. Such density can be achieved if the metal tube of the resistance heating element is based on steel or stainless steel. The mechanical strength of the tube material limits the density of the powder that can be obtained by compression. At heating elements having the tube made from a soft material, for example copper, the insulating material can not be compressed to a density of the powder higher than 3.0 g/cm^3. These can be used only at low temperatures.

Relatively to the insulation resistance, the average temperature inside the heater insulating layer must be maintained as low as possible, in order to prevent high leakage currents.

Thermal conductivity of the insulation material has decisive influence both on the working temperature of the resistive material and on the temperature difference between the heating coil and tube at a given temperature of the tube. A high thermal conductivity of the insulating material causes a lower temperature of the heating coil and thus, a lower average temperature of the insulation. A lower temperature of the resistive wire means a longer life, and a smaller average temperature of the insulation results in lower leakage current, so a safer operation.

The bending radius has a great influence on the thermal conductivity due to the fact that while bending, the density of the insulating material decreases in those places, worsening heat transmission. This disadvantage can be compensated by an additional pressing of the heating elements in the bended points.

While reducing the section of the filled tube, the most important changes are:

- tube elongation;
- increasing the density of the insulation material by compression compacting, which results in improving the transmission of heat from the heating coil to the tube. Note that a higher density of filler leads to better thermal conductivity and exaggerated

compression, in parallel with grinding grain of the filler that changes prescribed granularity of the dust, harms the thermal conductivity;

- reduced electrical resistance of the wire;

The proposed mathematical model was designed based on the drawing from Figure 3. The modeling mathematical equations were written to describe physical phenomena in four distinct areas: the outer metal tube, outer insulating layer (located between the metallic tube and electrical resistance), the inside insulating layer (located inside the spiral of the heating resistance) and electrical resistance itself.
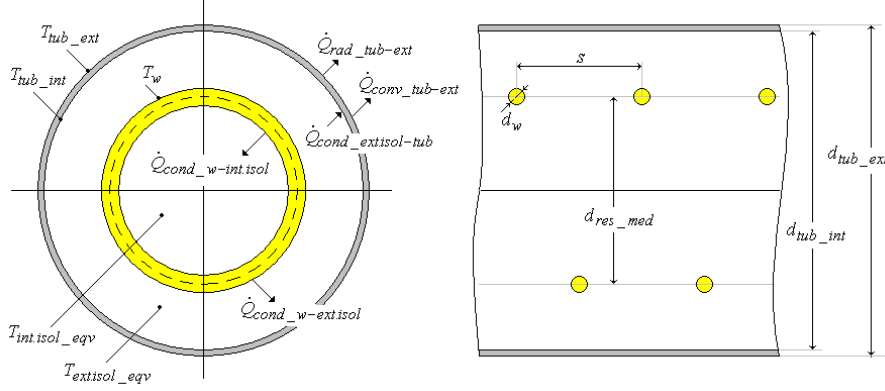

Fig.3. Resistance in tube – active zone

A. Mathematical Modeling and Simulation of the Metallic Tube

There are two possibilities of calculating the heat delivered to the exterior by the tubular heating element. The results of the total heat delivered by the tube are similar in the two calculation variants. In the first variant, we can consider the most general case in which the heating element generates heat to the environment both through convection heat flow ($\dot{Q}_{conv\_tub-ext}$) and by radiation heat flow ($\dot{Q}_{rad\_tub-ext}$). In the metal tube, the heat flow received by conduction from the insulating material from the layer separating the resistor from the tube ($\dot{Q}_{cond\_ext.isol-tub}$) is partially stored ($\dot{Q}_{store\_tub}$), the rest being transferred to the exterior environment. The equations describing these phenomena are:

$$\dot{Q}_{cond\_ext.isol-tub} = \dot{Q}_{store\_tub} + \dot{Q}_{out\_tub} \; [\text{W}] \quad (1)$$

$$\dot{Q}_{out\_tub} = \dot{Q}_{rad\_tub-ext} + \dot{Q}_{conv\_tub-ext} \; [\text{W}] \quad (2)$$

$$\dot{Q}_{rad\_tub-ext} = \varepsilon \cdot C_n \cdot S_{tub\_ext} \cdot \left(T_{tub\_ext}^4 - T_0^4\right) [\text{W}](3)$$

$$\dot{Q}_{conv\_tub-ext} = \alpha_{ext} \cdot S_{tub\_ext} \cdot \left(T_{tub\_ext} - T_0\right) [\text{W}] \quad (4)$$

where: ε = the emissivity of the tube;
C_n = Ştefan-Boltzmann's constant [W·m⁻²·K⁻⁴];
α_{ext} = convective heat transfer coefficient from tub to environment [W·m⁻²·K⁻¹];

In the second variant, we can use the specific power of the outer surface of the tube.

Regardless of the variant, we can write:

$$\dot{Q}_{out\_tub} = \frac{T_{tub\_int} - T_{tub\_ext}}{R_{therm\_tub}} =$$

$$= \frac{2\pi \cdot L_{tub} \cdot \lambda_{tub}}{\ln\left(\dfrac{d_{tub\_ext}}{d_{tub\_int}}\right)} \cdot \left(T_{tub\_int} - T_{tub\_ext}\right) [\text{W}] \quad (5)$$

$$Q_{store\_tub} = m_{tub} \cdot c_{tub} \cdot \left(T_{tub\_eqv} - T_0\right) [\text{J}] \quad (6)$$

where: m_{tub} = the mass of the tube [kg]
c_{tub} = specific heat capacity of the tube material [J·kg⁻¹·K⁻¹].

T_{tub_eqv} = equivalent temperature of the tube calculated according to the equations from [29]:

$$T_{tub\_eqv} = T_{tub\_ext} + K_{tub} \cdot \left(T_{tub\_int} - T_{tub\_ext}\right) [\text{K}](7)$$

$$K_{tub} = \frac{1}{2 \cdot \ln\left(\dfrac{d_{tub\_ext}}{d_{tub\_int}}\right)} - \frac{1}{\left(\dfrac{d_{tub\_ext}}{d_{tub\_int}}\right)^2 - 1} \quad (8)$$

Figure 4 shows the model of the four main functional blocks that build up the Simulink model of the resistive heating element in a metallic tube. It is designed based on equations (5)-(8). Three external prescription blocks are attached to three inputs, and they provide:

- the product between the mass and the specific calorific capacity of the tube, calculated with the equation:

$$m_{tub} \cdot c_{tub} = \frac{\pi}{4}\left(d_{tub\_ext}^2 - d_{tub\_int}^2\right) \cdot L_{tub} \cdot \gamma_{tub} \cdot c_{tub} \quad (9)$$

- the thermal resistance of the metallic tube calculated from:

$$1/R_{therm\_tub} = \frac{2\pi \cdot L_{tub} \cdot \lambda_{tub}}{\ln\left(\dfrac{d_{tub\_ext}}{d_{tub\_int}}\right)} \qquad (10)$$

- the coefficient used to calculate the equivalent temperature of the metallic tube from the equation (8).
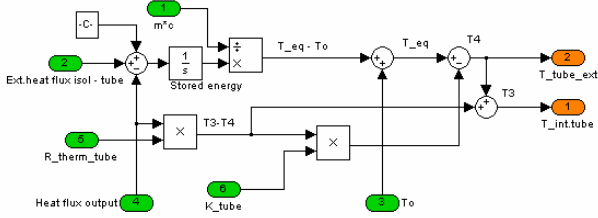

Fig. 4. The Simulink model of the metal tube

The block supplies two temperatures from the output. The momentary value of the temperature inside the metallic tube is used in the heat transfer calculations performed in the simulation block of the insulating material between the resistive spiral and the metallic tube. The instantaneous value of the temperature at the outer surface of the metallic tube is the one that determines the heat flow provided by the heating element to the environment in which it operates. This value allows the evaluation of the heat flow transferred to the exterior by convection and radiation.

The originally developed Matlab-Simulink model was based on equations (1) - (4). These two flows were used for the heat transfer to the exterior. We have subsequently modified the simulation system for calculating the heat provided by the heater, and we have used a technical date that any manufacturer puts on the datasheet. This is the specific power of the outer surface of the tube. The obtained results were almost identical. The model presented in this paper uses the second variant, which has the advantage of a simpler simulation scheme.

In the structural diagram from Figure 3, it is noted that the outside temperature of the tube is used to calculate (by means of an interpolation block) the specific emission power at the surface of the tube. This multiplies with the surface of the tube and yields the power caved to outside. The surface of the tube is a fixed parameter that is calculated before the simulation and is inserted into a prescription block. The multiplication value 10^4 ensures the passage of the emission power of the tube from W/cm² to W/m², considering that the surface of the tube was calculated in m².

B. Mathematical Modeling and Simulation of the Outer Insulating Layer (between resistive spiral and metallic tube)

The heat from the resistive element reaches the outer metallic tube passing through outer insulating layer by heat conduction. The thermal flow that passes through the thermal insulation layer ($\dot{Q}_{in\_ext.isol}$) is the sum between the heat flow taken directly over the surface of the resis-

tance by the outer insulating layer ($\dot{Q}_{cond\_w-ext.isol}$) and the one that is transferred from the inner insulating layer ($\dot{Q}_{cond\_int.isol-ext.isol}$). When modeling, it was considered that the heat flow provided by the resistance is divided equally between the inner and outer insulating layer.

$$\dot{Q}_{in\_ext.isol} = \dot{Q}_{cond\_w-ext.isol} + \dot{Q}_{cond\_int.isol-ext.isol} \, [W] \quad (11)$$

The heat flow that reaches the outer insulating layer is partially transmitted to the metal tube ($\dot{Q}_{cond\_ext.isol-tub}$) and the rest turns into heat gained in this layer ($Q_{store\_ext.isol}$).

$$\dot{Q}_{in\_ext.isol} = \dot{Q}_{store\_ext.isol} + \dot{Q}_{cond\_ext.isol-tub} \, [W] \quad (12)$$

Using the calculation method described in [29], we can determine the equivalent temperature of the outer insulating layer:

$$T_{ext.isol.\_eqv} = T_{tub\_int} + K_{ext.isol} \cdot \left(T_{ext.isol\_int} - T_{tub\_int}\right) [K] \quad (14)$$

$$K_{ext.isol} = \frac{1}{2 \cdot \ln\left(\dfrac{d_{tub\_int}}{d_{res.\_med}}\right)} - \frac{1}{\left(\dfrac{d_{tub\_int}}{d_{res.\_med}}\right)^2 - 1} \quad (15)$$

The thermal flow transferred to the metallic tube is:

$$\dot{Q}_{cond\_ext.isol-tub} = \frac{T_{ext.isol\_int} - T_{tub\_int}}{R_{therm\_ext.isol}} =$$
$$= \frac{2\pi \cdot L_{tub} \cdot \lambda_{isol}}{\ln\left(\dfrac{d_{tub\_int}}{d_{res\_med}}\right)} \cdot \left(T_{ext.isol\_int} - T_{tub\_int}\right) =$$
$$= K_{Rt\_ext.isol} \cdot \lambda_{isol} \cdot \left(T_{ext.isol\_int} - T_{tub\_int}\right)$$
$$(16)$$

The thermal conductivity depends strongly on the temperature and it was separated from the thermal resistance expression of outer insulation. It can be determined from tables or curves. For simulation, it can be approximated by using a polynomial interpolation type:

$$\lambda_{isol}\left(T_{ext.isol\_eqv}\right) = a_1 \cdot T^3_{ext.isol\_eqv} + a_2 \cdot T^2_{ext.isol\_eqv} + $$
$$+ a_3 \cdot T_{ext.isol\_eqv} + a_4 \quad (17)$$

The heat flow $\dot{Q}_{cond\_int.isol-ext.isol}$ in W can be determined accurately enough with the following relationships, where K_{16} depends on the contact area between the outer and inner insulation.

$$\dot{Q}_{cond\_int.isol-ext.isol} = K_{16} \cdot \lambda_{isol} \cdot \left(T_{int.isol\_eqv} - T_{ext.isol\_eqv}\right) \quad (18)$$

where $\lambda_{isol} = \lambda_{isol}\left(\dfrac{T_{ext.isol\_eqv} + T_{int.isol\_eqv}}{2}\right)$ measured in [W·m⁻¹·K⁻¹] is approximated similarly with (17) and

$$K_{16} = \cfrac{2\pi \cdot \left(\cfrac{L_{tub}}{s} \cdot (s - d_w) \right)}{\ln\left| \cfrac{\cfrac{d_{tub\_int}}{2\sqrt{e}} \cdot \left(\cfrac{d_{tub\_int}}{d_{res\_med}} \right)^{\cfrac{d^2_{res\_med}}{d^2_{tub\_int} - d^2_{res\_med}}}}{\cfrac{d_{res\_med}}{2 \cdot \sqrt{e}}} \right|} \quad [m] \, (19)$$

The Simulink model is shown in Figure 5. The temperature-dependent quantities for this functional block are the specific heat capacity of the insulating material and the thermal conductivity of the insulating material. For them, linear interpolation blocks were provided in the model.
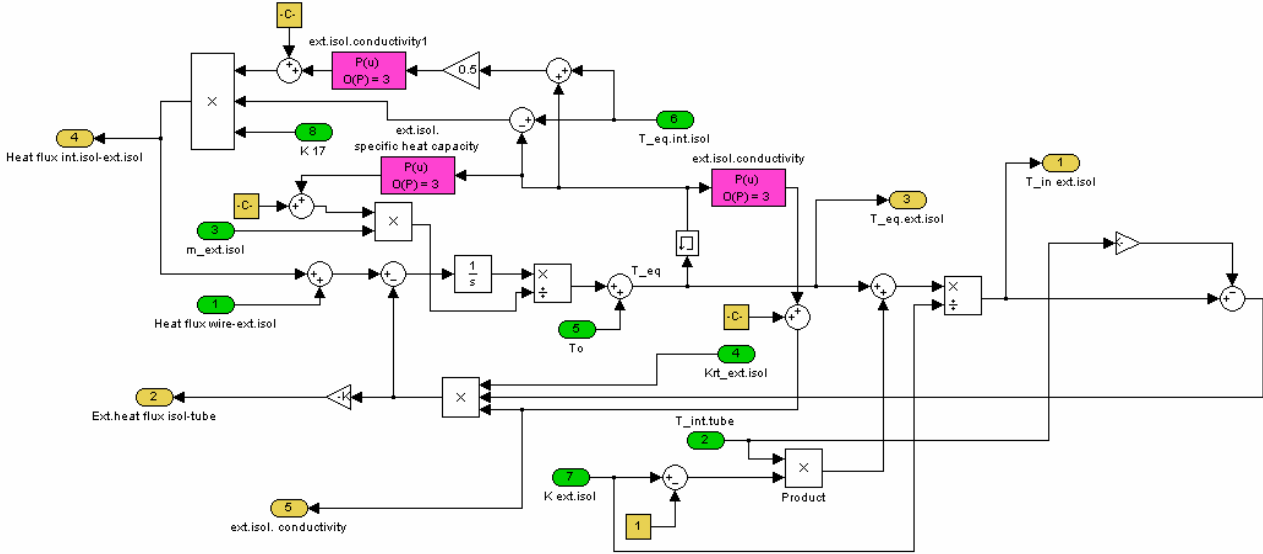

Fig. 5.   The Simulink model of the insulating material from outside the resistive spiral

The Simulink model of this functional block is complemented with four external prescription blocks (Fig.9), which provide four pre-calculated simulation sizes, namely:

- the mass of the insulating material between the resistive spiral and the metal tube, calculated with the relation:

$$m_{ext.isol} = \frac{\pi}{4}\left(d^2_{tub\_int} - d^2_{res\_med} \right) \cdot L_{tub} \cdot \gamma_{isol} \quad (20)$$

- the coefficient which characterizes the thermal flux between the insulating material and the outer tube:

$$K_{Rt\_ext.isol} = \frac{2\pi \cdot L_{tub}}{\ln\left| \cfrac{d_{tub\_int}}{d_{res\_med}} \right|} \quad (21)$$

- the coefficient used to calculate the equivalent temperature of the outer insulating layer, calculated with the equation (15);
- the coefficient which is used to determine the heat exchange between the inner insulating layer and the outer insulating layer calculated with the equation (19).

From Figure 9 it can be seen that this functional block plays an essential role in the model, being interconnected with all three other main blocks. These connections are made due to the fact that the outer insulating layer is the one that transfers the thermal flows from the resistive element and the insulator from inside the resistive spiral to the outer metal tube.

C. *Mathematical Modeling and Simulation of the Inside Insulating Layer (inside the resistive spiral)*

The insulating inner layer has the physical role of maintaining the resistive spiral shape inside during the deforming process of the tube by reducing its section. This layer receives half of the heat flow ceded by the resistance ($\dot{Q}_{cond\_w-int.isol}$). It uses one part to heat itself ($Q_{store\_int.isol}$) and gives the rest to the metal tube through the outer insulating layer ($\dot{Q}_{cond\_int.isol-ext.isol}$).

$$\dot{Q}_{cond\_w-int.isol} = \dot{Q}_{store\_int.isol} + \dot{Q}_{cond\_int.isol-ext.isol} \quad (22)$$

$$Q_{store\_int.isol} = m_{int.isol} \cdot c_{isol} \cdot \left(T_{int.isol\_eqv} - T_0 \right) \; [J] \quad (23)$$

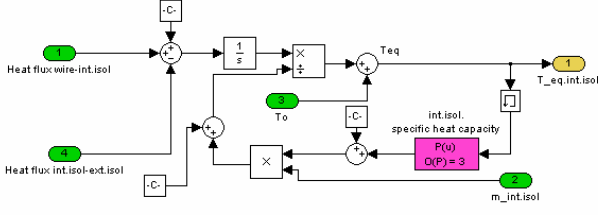The Simulink model of this block is presented in Fig.6.

Fig. 6. The Simulink model of the insulated material from inside the resistive spiral

This model is the simplest of the component blocks of the tube resistive heater element model. There is only one external prescription block that provides the pre-calculated value of the mass of the insulating material from inside the spiral conductor. It is calculated before the simulation with the equation:

$$m_{int.isol} = \frac{\pi}{4} \cdot d_{res\_med}^2 \cdot L_{tub} \cdot \gamma_{isol} \qquad (24)$$

The specific heat capacity of the insulating material is a function of its equivalent temperature, defined as in [29]. Regarding the same insulating material inside and outside the conductor spiral, the interpolation polynomials used in various blocks have the same coefficients. It differs only the size applied to the input of the linear interpolation block.

D. *Mathematical Modeling and Simulation of the Resistor*

Mathematical equations that model the heat resistance are based on the quantities characteristic for the electricity to be converted into heat. Usually, a resistive tubular heater has the inductance in the range $L \in \left[1...10^2\right] \mu H$. At the industrial frequency (50 Hz) the inductive reactance is of the order $X_L \in \left[10^{-3}...10^{-1}\right] \Omega$ and can be neglected in relation with electrical resistance. The current drawn from the power supply:

$$i(t) = \frac{u(t)}{R_w(t)} \text{ [A]} \qquad (25)$$

It is considered that the heating is performed at constant voltage and the current absorbed in transient regime by the resistive element is modified due to resistance dependence of the temperature.

$$R_w(t) = R_{w\_0} \cdot K_w(\Delta T_w(t)) \text{ [}\Omega\text{]} \qquad (26)$$

$$\Delta T_w(t) = T_w(t) - T_0 \text{ [K]} \qquad (27)$$

where T_0 is the temperature of the resistor before starting the heating process.

In the previous set of equations is highlighted the dependence of electrical resistance on its temperature. This dependence can be modeled mathematically by using a polynomial interpolation created based on information provided by the manufacturer of resistive wire.

$$K_w(\Delta T_w(t)) = b_1 \cdot (\Delta T_w(t))^3 + b_2 \cdot (\Delta T_w(t))^2 + b_3 \cdot (\Delta T_w(t)) + b_4 \qquad (28)$$

The electric power converted at a given time is used for self-heating of the resistance ($\dot{Q}_{store\_w}$), or is disposed on the inside insulating layer ($\dot{Q}_{cond\_w-int.isol}$) and the outer insulating layer ($\dot{Q}_{cond\_w-ext.isol}$).

$$P = U \cdot I = \dot{Q}_{cond\_w-ext.isol} + \dot{Q}_{cond\_w-int.isol} + \dot{Q}_{store\_w} \qquad (29)$$

$$\dot{Q}_{cond\_w-ext.isol} = \frac{2\pi \cdot \left(\frac{L_{tub}}{s} \cdot \left(\frac{\pi \cdot d_w}{2}\right)\right)}{\ln\left(\frac{d_{tub\_int}}{d_{res\_med}}\right)} \cdot \lambda_{isol} \cdot (T_w - T_{tub\_int}) =$$
$$= K_{26} \cdot \lambda_{isol}(T_{ext.isol\_eqv}) \cdot (T_w - T_{tub\_int}) \qquad (30)$$

where: $\lambda_{isol} = \lambda_{isol}(T_{ext.isol\_eqv})$ [W·m^{-1}·K^{-1}].

$$\dot{Q}_{cond\_w-int.isol} = \frac{2\pi \cdot \left(\frac{L_{tub}}{s} \cdot \left(\frac{\pi \cdot d_w}{2}\right)\right)}{\ln\left|\frac{\frac{d_{res\_med}}{2}}{\frac{d_{res\_med}}{2 \cdot \sqrt{e}}}\right|} \cdot \lambda_{isol} \cdot (T_w - T_{int.isol\_eqv}) =$$
$$= K_{27} \cdot \lambda_{isol}\left(\frac{T_{int.isol\_eqv} + T_w}{2}\right) \cdot (T_w - T_{int.isol\_eqv}) \qquad (31)$$

where: $\lambda_{isol} \cong \lambda_{isol}\left(\frac{T_{int.isol\_eqv} + T_w}{2}\right)$ [W·m^{-1}·K^{-1}].

The thermal flow used for self-heating of the resistance:

$$\dot{Q}_{store\_w} = \frac{\mathbf{d}}{\mathbf{d}t}\left(m_w \cdot c_w(T_w(t)) \cdot \Delta T_w(t)\right) \qquad (32)$$

where the specific heat capacity depends on the temperature:

$$c_w(T_w(t)) = c_1 \cdot (T_w(t))^3 + c_2 \cdot (T_w(t))^2 + c_3 \cdot (T_w(t)) + c_4 \qquad (33)$$

The equations (25)-(33) are used for the Simulink model shown in Figure 7. To determine the value of the electrical resistance at different operating temperatures, the value of the cold resistance (as in Figure 9) is introduced from an external prescription block. This value is permanently corrected according to the momentary temperature of the resistive wire by multiplying with the value provided by the three-point linear interpolation block "Coef R - Kw (b)"(Fig.7). The other sizes introduced from the outside through prescription blocks are the mass of the resistive wire and the coefficients K_{26} and K_{27}. These sizes are calculated before the start of the simulation based on the primary physical quantities of the heating element in tube, listed above. Their calculation formulas can be determined by analyzing equations (30), (31) and (32) and these are:

$$m_w = \frac{\pi}{4} \cdot d_w^2 \cdot L_w \cdot \gamma_w = \frac{\pi}{4} \cdot d_w^2 \cdot \frac{L_{tub}}{s} \cdot \pi \cdot d_{res\_med} \cdot \gamma_w \qquad (34)$$

$$K_{26} = \frac{2\pi \cdot \left(\frac{L_{tub}}{s} \cdot \left(\frac{\pi \cdot d_w}{2} \right) \right)}{\ln\left(\frac{d_{tub\_int}}{d_{res\_med}} \right)} \qquad (35)$$

$$K_{27} = \frac{2\pi \cdot \left(\frac{L_{tub}}{s} \cdot \left(\frac{\pi \cdot d_w}{2} \right) \right)}{\ln\left(\frac{\frac{d_{res\_med}}{2}}{\frac{d_{res\_med}}{2 \cdot \sqrt{e}}} \right)} = 4\pi \cdot \left(\frac{L_{tub}}{s} \cdot \left(\frac{\pi \cdot d_w}{2} \right) \right) \qquad (36)$$

It can be seen that the Simulink model of Figure 7 takes into consideration that during the thermal regime the specific heat capacity of the resistive material and the thermal conductivity of the insulating material are changing. For these as well as for the coefficient of calculating the electrical resistance, interpolation polynomials are calculated based on tabulated data or based on curves provided by the producers of the respective materials. In all cases, it was chosen for ordering polynomials of order 3 that adequately approximate the temperature dependencies.

For the resistance coefficient calculation and for the heat capacity specific to the resistive material the values are related to the momentary temperature of the resistive wire. For the thermal conductivity used to determine the heat flow changed by the resistance with the insulating material, the values are obtained in relation to the average between the temperature of the resistive wire and the equivalent temperature of the insulating material within the resistive spiral.
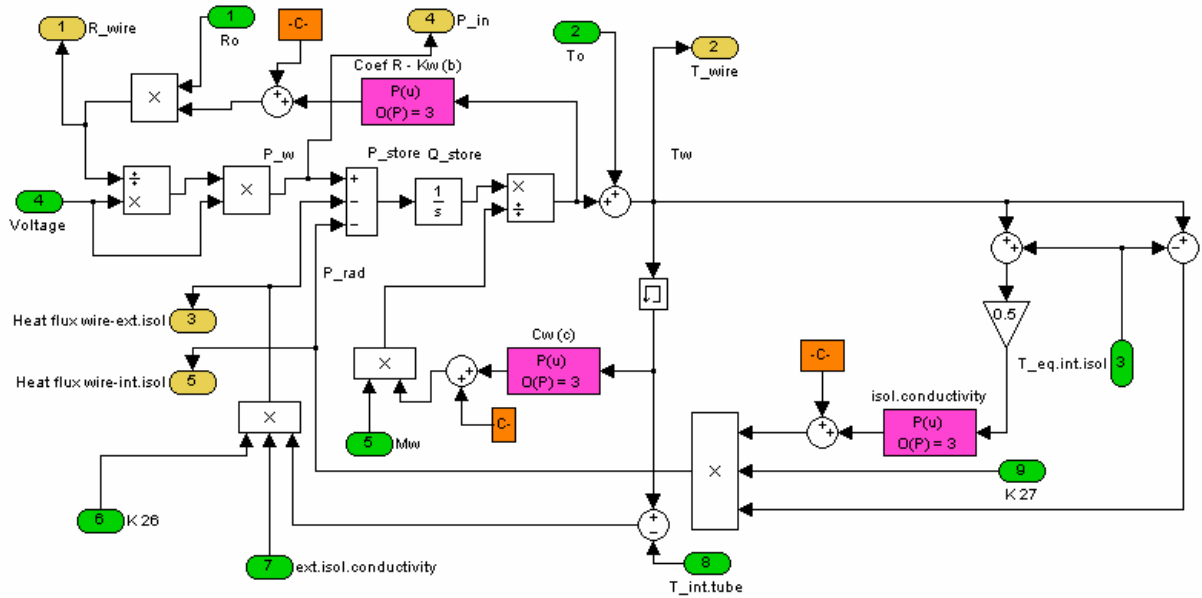

Fig. 7. The Simulink model of the resistive element

E. The Overall Matlab-Simulink Model

The overall model was conceived as a block that can be used as a whole in various applications that contain resistive heating elements in tube (Figure 8). It has two external inputs (operating voltage-RMS value and the ambient temperature before the start of the heating process). At the output, it provides five information regarding the temperature in various internal areas of the heating element, the value of the electrical resistance, and two information about the electrical power consumed and ceded by the heating element respectively. Its internal structure is shown in Figure 9.

In the assembly shown in Figure 9, it can be observed the four main blocks, which simulate: the resistive element itself, the insulating material found inside the resistive spiral, the insulated material between the metallic tube and the resistive spiral. A number of prescription blocks can also be seen. Most values that are loaded in these prescription blocks are calculated before simulation, based on measured basic parameters.
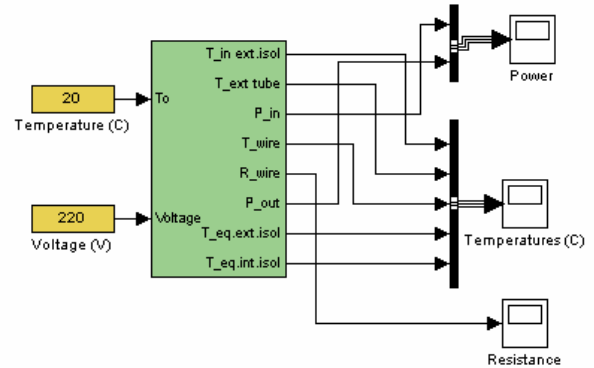

Fig. 8.   Heating resistive element in tube

A number of six blocks have a fixed inserted value of 273.15 and are useful to provide the conversion between the Celsius and Kelvin temperature scales. It will return

with the description of the four basic functional blocks and the values contained in each of the prescription blocks. Figure 9 shows how each of these four blocks is interconnected to simulate the assembly of the resistive element in tube.
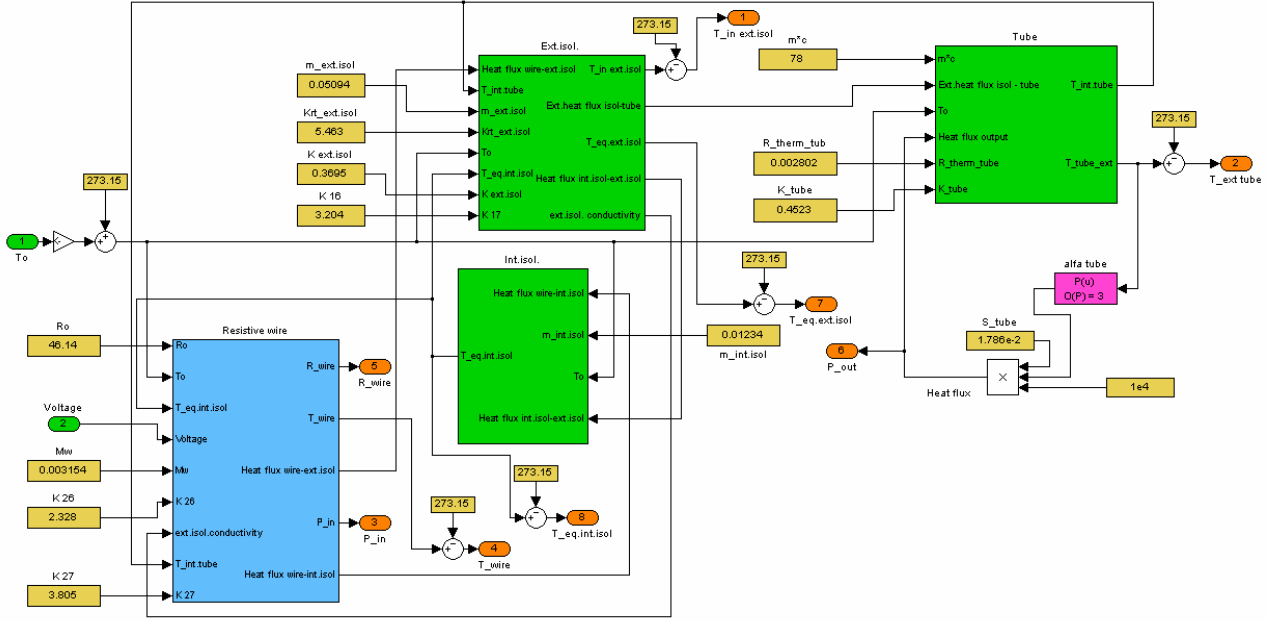

Fig. 9.   The model structure of resistive heating element in tube

For the practical use of the proposed mathematical model it is necessary to measure or to determine, by calculation, some primary parameters of the simulated resistor in tube. These are: the resistive wire diameter (d_w), the average diameter of the conductive spiral (d_{res_med}), the winding step (s), the length of the tube (L_{tub}), the inside diameter of the metal tube (d_{tub_int}), the outside diameter of the tube (d_{tub_ext}), the value of the cold resistance (R_{w_0}), the specific weight of the insulating material (γ_{isol}), the specific heat capacity of the insulating material (c_{isol}), the specific weight of the metal tube (γ_{tub}), the specific heat capacity of the metal tube (c_{tub}), the thermal conductivity of the metal tube (λ_{tub}), the outer convection coefficient of the metal tube (α_{ext}), the emisivity of the tube (ε), the thermal conductivity of the insulating material (λ_{isol}), and the specific weight of the resistive conductive material (γ_w).

IV. SIMULATION RESULTS

The verification of the proposed simulation model was carried out for a resistive heating element in tube having a supply voltage of 220V a.c. and power of 1000W. From its technical datasheet we could find out that the tube is made of Nikrothal N2R, it can operate at a maximum temperature of 900ºC and at a temperature of 700ºC the specific power supplied is 5.6W/cm². By connecting it to the 220V/50Hz monophase voltage network, the measured temperature was stabilized at about 680ºC. The resistance and inductance were determined in the cold state, by measuring them at ambient temperature.

Since the inductive reactance calculated on the basis of the measured inductance is about 1mΩ, it can be neglected in relation to the resistance which at 20ºC is 46.14Ω. The length and outer diameter of the tube were also measured. Subsequently, the heating element was cut to determine the other constructive dimensions required for the simulation and which were mentioned at the end of Section III. It is known from the product datasheet that the resistance is made of Kanthal type A and the insulating material is made of magnesium oxide. The necessary data on these materials, as well as on the tube material were found on the internet.
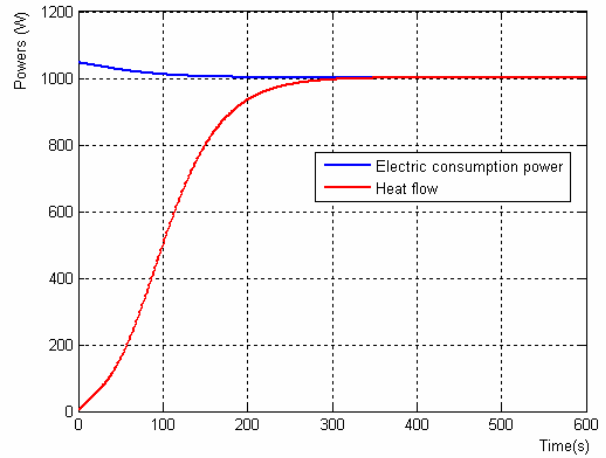

Fig. 10.   The electric consumption power and the heat flow evolution

Figure 10 shows the evolution of powers absorbed from the power supply network and supplied at the output as a

heat flux. They can be seen their equalization in the stationary regime.

A transient regime of heating the resistive element was simulated for 10 minutes. The curves obtained indicate that in air, the resistive element enters in stationary mode after about 8 minutes, i.e. it has a much higher inertia than a spiral resistive element in the air.

Figure 11 shows the change of the value of the electrical resistance as the resistive element heats up.
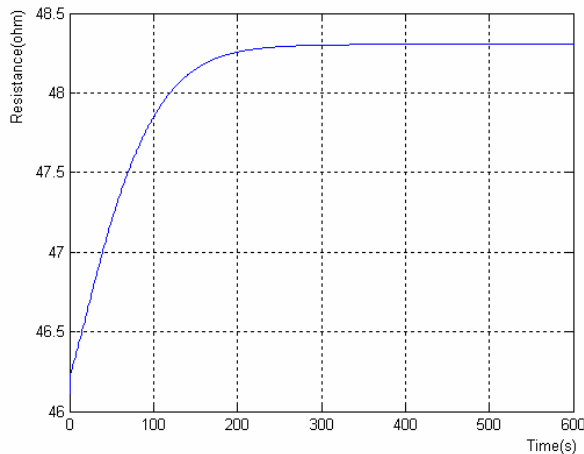

Fig. 11. The resistance time evolution

The last figure shows the evolution of temperatures at various points of the heating element in:
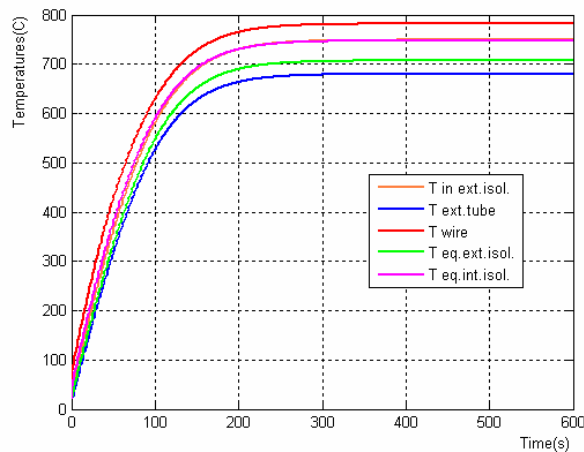

Fig. 12. The evolution of temperatures of the heating element in various points

It can be seen that the difference between resistance temperature curve (highest) and the temperature of the tube (the lower curve) is becoming stable at arround 110ºC. Each of these temperatures is lower than the maximum permissible temperature.

V. CONCLUSIONS AND WORKING PERSPECTIVES

The mathematical model proposed was created to provide a basis for achieving a numerical simulation model. It will be able to provide analyzes in steady or transient regime. Different situations can be simulated and we can obtain results that allow better design of household or industrial installations equipped with electrical heating elements with resistance in tube.

To model a steady operating regime, the mathematical model can be simplified by switching from temperature dependent parameters to constant parameters. In this situation, one can try to define some transfer functions for each of the four areas, or even a single one for the element with electrical heating in tube.

Regarding future activities, it is contemplated to perform a simultaneous simulation of a winding resistor in the air and a heater element in the tube, in order to compare their specific thermal inertia. On the other hand, it is envisaged to use the proposed simulation model for resistors in tube reinforced in metal plates, such as the iron or the coffee maker.

REFERENCES

[1] Kanthal AB. , "Kanthal Handbook – Heating Alloys for Electric Household Appliances", Box 502, SE-73427 Hallstahammar, Sweden

[2] http://www.cetal.com/

[3] http://www.omega.com/subsection/tubular-heaters-all.html

[4] http://www.kanthal.com/en/products/

[5] http://www.tempco.com/Tubular/tubular_hub.htm

[6] WATTCO™, "Tubular Heaters - immersion heaters"

[7] Kanthal AB, "Kanthal super – Electric Heating Element Handbook", Sweden, ISBN:91-86720-08-2

[8] M.I. Neacă, A.M. Neacă, "Mathematical Modeling and Simulation of an Automatic Electric Heating System", Proceedings of the 19th International Conference on Systems (part of CSCC '15), Zakynthos Island, July 16-20, 2015, Greece, published in volume: RECENT ADVANCES in SYSTEMS, ISSN: 1790-5117,(Advances in automatic control) ISBN: 978-1-61804-321-4.

[9] I. Neacă, A.M. Neacă, "The Modeling of the Heating Resistors in Transient Regime", Journal of Materials Science and Engineering B, Volume 1, Number 2, July 2011 (Serial Number 2), ISSN 2161-6221, pag.170-177, David Publishing Company, 1840 Industrial Drive, Suite 160, Libertyville, Illinois 60048.

[10] A.Bejan, A.D.Kraus: Heat Transfer Handbook; John Wiley &Sons, Inc., 2003

[11] F.P.Incropera, D.P.DeWitt, T.L.Bergman, A.S.Lavine: Fundamentals of Heat and Mass Transfer; John Wiley &Sons, Inc., 2007

[12] L.M.M. Tijskens, M.L.A.T.M. Hertog, B.M. Nicolai, Food Process Modelling, Woodhead Publishing Series in Food Science, Technology and Nutrition, Volume 59 from Woodhead Publishing in food science and technology, Woodhead Publishing, 2001, ISBN: 978-1-85573-565-1

[13] J.H. Lienhard IV, J.H. Lienhard V, A heat transfer textbook, Published by J.H. Lienhard V, 2000, Cambridge, Massachusetts, U.S.A.

[14] M. Sen, Analytical Heat Transfer, Doctor thesis, Department of Aerospace and Mechanical Engineering, University of Notre Dame, March, 2015

[15] D. Marlow, Mathematical modeling of the heat treatment in the continuous processing of stell strip, Doctor of Philosophy thesis, Department of Mathematics, University of Wollongong,1995, http://ro.uow.edu.au/theses/1552

[16] E.Pereira-Leite, Matlab - Modelling, Programming and Simulations, Sciyo, Croatia, 2010, ISBN 978-953-307-125

[17] C. Wannagosit, P. Sakulchangsatjatai, N. Kammuang-lue, P. Terd-toon, Validated mathematical models of a solar water heater system with thermosyphon evacuated tube collectors, Case Studies in Thermal Engineering 12 (2018), Elsevier, pg. 528–536

[18] ***, Dimensioning and design of solar thermal systems, AEE – Institute for Sustainable Technologies, Feldgasse 19, A-8200 Gleisdorf, Austria

[19] R. Santa, L. Garbai, The mathematical model and numerical simulation of the heat pump system, ANNALS OF FACULTY ENGINEERING HUNEDOARA – International Journal Of Engineering, Tome XI(Year 2013)-Fascicule 4(ISSN:1584-2673)

[20] D. Taler, M. Trojan, J. Taler, Mathematical modeling of tube heat exchangers with complex flow arrangement, Chemical and Process Engineering 2011, 32 (1), DOI: 10.2478/v10176-011-0001-y, pg. 7-19

[21] M. Yadav, N.K. Saikhedkar, Simulation modelling for the performance of evacuated tube solar collector, International Journal of Innovative Research in Science, Engineering and Technology, Vol. 6, Issue 4, April 2017, ISSN: 2319-8753, pg. 5634-5642

[22] M.A. Sabiha, R. Saidur, S. Mekhilef , O. Mahian, Progress and latest developments of evacuated tube solar collectors, RenewableandSustainableEnergyReviews51(2015), Elsevier, pg.1038–1054

[23] P.Y. Wang, H.Y. Guan, Z.H. Liu, G.S. Wang, F. Zhao, H.S. Xiao, High temperature collecting performance of a new all-glass evacuated tubular solar air heater with U-shaped tube heat exchanger, Energy Conversion and Management 77 (2014), Elsevier, pg. 315–323

[24] A. Aboulmagd, A. Padovan, R. De Césaro Oliveski, D. Del Col, A New Model for the Analysis of Performance in Evacuated Tube Solar Collectors, 3rd International High Performance Buildings Conference, Purdue, July 14-17, 2014, Paper 142

[25] A.M. Saleh, Modeling of flat-plate solar collector operation in transient states, Thesis for Master of Science in Engineering, May 2012, Purdue University, Fort Wayne, Indiana

[26] P. Mastny, J. Moravek, J. Pitron, Mathematical modeling of basic parts of heating systems with alternative power sources, Recent Advances in Fluid Mechanics and Thermal Engineering, ISBN: 978-1-61804-311-5, pg.126-131

[27] M. Yadav, N.K. Saikhedkar, Simulation modelling for the performance of evacuated tube solar collector, International Journal of Innovative Research in Science, Engineering and Technology, Vol. 6, Issue 4, April 2017, ISSN: 2319-8753, pg. 5634-5642

[28] T. Lazăr, N. Petre, "Elemente încălzitoare electrice în tuburi metalice", Ed.Tehnică Bucureşti

[29] M.I. Neacă, A.M. Neacă, "The Quick Estimation of the Stored Heat in a Cylindrical Wall", Proceedings of the 2015 International Conference on Pure Mathematics, Applied Mathematics and Computational Methods (PMAMCM 2015), Zakynthos Island, July 16-20, 2015, Greece, published in volume: RECENT ADVANCES in MATHEMATICS, ISSN: 2227-4588 (Mathematics and computers in science and engineering series), ISBN: 978-1-61804-323-8, pag. 57 – 60.